applied sciences

MDPI

Article

A Sub-Mother UAV Swarm Deployment and Routing for Power Grid Emergency Communication

Youfang Gu [1], Yu Song [1], Minkun He [1], Junchen Li [1], Shun Yang [1], Xinyue Li [1], Yao Zhao [2], Changxin Liu [3,*], Ye Xiang [3] and Wei Yue [3,*]

[1] Xingyi Power Supply Bureau of Guizhou Power Grid Co., Ltd., China Southern Power Grid Co., Ltd., JuShan Avenue, Xingyi 562400, China
[2] Liupanshui Power Supply Bureau of Guizhou Power Grid Co., Ltd., China Southern Power Grid Co., Ltd., No. 45 Zhongshan Middle Road, Liupanshui 553001, China
[3] Marine Engineering College, Dalian Maritime University, Dalian 116026, China
* Correspondence: liu_changxin@dlmu.edu.cn (C.L.); weiy@dlmu.edu.cn (W.Y.)

Abstract

This paper investigates the coordinated deployment and routing of communication equipment by a Sub-mother UAV swarm in power-grid emergency communication scenarios. Considering mission timeliness and payload constraints, a heterogeneous MUAV–SUAV coordinated deployment-and-routing model is established to minimize the total system cost, including platform flight cost, SUAV activation cost, and penalty cost caused by delayed deployment. To solve this problem, a two-stage optimization framework is proposed. In the first stage, an improved K-means clustering algorithm with neighborhood search (K-means-NS) is developed to divide deployment points into feasible sub-regions while satisfying SUAV endurance constraints and maintaining the deployment–retrieval payload balance required by the MUAV. In the second stage, the MUAV inter-region visiting sequence is treated as a routing subproblem, and an improved adaptive genetic algorithm (IAGA) is designed to optimize the coordinated routes of the MUAV and SUAVs within each sub-region. The IAGA adopts hybrid encoding, feasible-solution adjustment, elitist selection, and adaptive crossover–mutation operations to improve search efficiency under complex constraints. Numerical experiments on small-, medium-, and large-scale scenarios show that the proposed method can generate feasible sub-region divisions and coordinated routing schemes. Compared with GA and G-PSHA, IAGA reduces the total flight cost by approximately 21.2%, 10.5%, and 23.2% relative to GA and by approximately 0.2%, 2.5%, and 8.1% relative to G-PSHA in the three scenarios, respectively. Sensitivity analysis further indicates that stricter mission-timeliness requirements increase penalty costs, highlighting the importance of timely communication-device deployment in emergency restoration.

Keywords: sub-mother UAV swarm; power grid emergency communication; deployment and routing; improved K-means clustering; improved adaptive genetic algorithm

Academic Editor: Rui Araújo

Received: 20 March 2026
Revised: 20 June 2026
Accepted: 25 June 2026
Published: 1 July 2026

1. Introduction

In recent years, extreme natural disasters such as earthquakes, floods, and ice storms have frequently damaged power infrastructure and communication networks, creating serious challenges for emergency repair and grid restoration [1,2]. In post-disaster power-grid scenarios, temporary communication equipment must be rapidly deployed to support repair command, on-site information backhaul, and emergency decision-making [3,4].

However, damaged roads, disrupted traffic, and inaccessible repair sites often make conventional ground-based communication support difficult to implement [5,6]. In addition, emergency communication tasks are usually subject to strict timeliness requirements, and delayed deployment may reduce the effectiveness of disaster-response operations [7,8]. Therefore, aerial emergency communication deployment has become an important solution for restoring communication services in disaster areas.

Sub-unmanned aerial vehicles (SUAVs) have advantages in high mobility, flexible vertical take-off and landing capability, and access to scattered task points, but their payload capacity and endurance are limited [9,10]. Mother unmanned aerial vehicles (MUAVs), in contrast, have stronger carrying capacity and longer endurance and can transport communication devices and multiple SUAVs to the disaster area [11–14]. A coordinated MUAV–SUAV system can therefore combine the long-distance transportation and carrying capability of the MUAV with the local flexible deployment capability of SUAVs. In the considered power-grid emergency communication scenario, the MUAV carries communication devices and SUAVs to the task area, while SUAVs perform local delivery and activation of communication devices. The MUAV also participates in inter-region movement, device replenishment, and retrieval operations. This coordinated mechanism is suitable for rapid communication restoration in no-signal or weak-signal areas [15,16].

The coordinated deployment and routing of MUAV–SUAV systems is related to several research streams, including UAV routing, heterogeneous fleet routing, truck–drone logistics, time-window routing, location-routing problems, and emergency communication deployment. Existing studies have investigated truck–drone cooperative delivery, two-echelon routing, drone scheduling, and route optimization under operational constraints [17–21]. Adaptive genetic algorithms have also been used for heterogeneous multi-UAV task assignment [22], while exact and heuristic approaches have been developed for multi-echelon drone-routing and truck–drone scheduling problems [23,24]. More specifically, Ref. [25] considers heterogeneous truck–drone cooperative delivery and pickup services. In addition, recent location-sizing and routing studies have shown the effectiveness of integrating location decisions with routing optimization in complex logistics systems [26]. However, most existing methods are designed for conventional logistics delivery or homogeneous vehicle routing settings. They usually do not jointly consider the deployment and retrieval of emergency communication devices, the dynamic payload evolution of a MUAV, SUAV activation cost, rendezvous coordination, and time-window penalties caused by delayed communication-device activation. These features make the present power-grid emergency communication problem different from standard vehicle routing or truck–drone delivery problems.

Compared with Ref. [25], the present problem introduces two additional couplings. First, the MUAV payload changes dynamically because communication devices are deployed and retrieved during the mission. This makes the feasibility of sub-region division dependent on the deployment–retrieval payload balance. Second, emergency communication devices must be deployed and activated within mission time windows; otherwise, penalty costs are incurred.

To address the above issues, this paper studies a heterogeneous MUAV–SUAV coordinated deployment-and-routing problem with payload constraints and mission time-window penalties. The objective is to minimize the total system cost, including platform flight cost, SUAV activation cost, and delayed-deployment penalty cost. The proposed framework is intended to provide decision support for power-grid emergency communication restoration by balancing deployment urgency, UAV resource allocation, and operational cost.

The main contributions of this paper are summarized as follows.

First, a heterogeneous MUAV–SUAV coordinated deployment-and-routing model is established for power-grid emergency communication scenarios. Different from conventional logistics routing models, the proposed model considers communication-device deployment and retrieval, MUAV payload evolution, SUAV dispatching, platform-dependent flight costs, and mission time-window penalties within a unified cost-minimization framework.

Second, a K-means clustering algorithm with neighborhood search (K-means-NS) is developed to generate feasible sub-regions before route optimization. The algorithm adjusts noise points through neighborhood search so that the generated sub-regions satisfy SUAV endurance constraints, SUAV payload constraints, and the MUAV deployment–retrieval payload balance. This provides feasible regional inputs for subsequent coordinated routing.

Third, an improved adaptive genetic algorithm (IAGA) is designed for coordinated MUAV–SUAV route optimization within and between sub-regions. The IAGA adopts hybrid encoding, feasible-solution adjustment, elitist selection, adaptive crossover–mutation operations, and a historical-improvement-based mutation operator. These mechanisms jointly optimize the MUAV visiting sequence and SUAV task assignment under coupled payload and time-window constraints.

The remainder of this paper is organized as follows. Section 2 describes the problem and formulates the heterogeneous MUAV–SUAV coordinated deployment-and-routing model. Section 3 presents the two-stage solution framework, including K-means-NS clustering and IAGA-based route optimization. Section 4 reports numerical experiments, algorithm comparisons, and sensitivity analysis. Section 5 concludes the paper and discusses future research directions.

2. Problem Description

This paper investigates the optimal cost problem for the coordinated deployment and necessary retrieval of communication equipment in disaster areas by MUAV collaborating with multiple SUAVs, under the dual constraints of mission timeliness and payload capacity. The total system cost primarily includes the MUAV's flight cost, the fixed dispatch cost for SUAVs, the SUAVs' flight cost, and penalty costs incurred due to deployment delays at deployment points. Therefore, the problem studied in this paper is defined as a heterogeneous MUAV–SUAV coordinated deployment-and-routing problem with payload constraints and mission time-window penalties. For consistency, the MUAV denotes the mother UAV, the SUAV denotes the sub-UAV, a deployment point denotes a task point where a communication device is delivered and activated, a retrieval point denotes a task point where an existing communication device is picked up, and a sub-region denotes a task area assigned for coordinated MUAV–SUAV operation.

The following modeling assumptions are adopted in this study:

The analytical description below follows a two-stage deployment-and-routing logic. The first stage divides the task area into feasible sub-regions. The second stage optimizes the coordinated routes of MUAVs and SUAVs within and across these sub-regions, as shown in Figure 1.

1. Each dispatch of a SUAV from the MUAV to execute a task incurs a fixed cost, regardless of the flight distance or duration.
2. The number of key devices retrieved by the unmanned platform within a sub-area and the number of new devices to be deployed must satisfy a dynamic payload and capacity balance constraint for the platform.
3. The deployment time of the MUAV or SUAV at any deployment point must be completed within the specified time window; exceeding this window incurs a corresponding penalty cost.

4. To simplify the model, both the MUAV and SUAVs are assumed to fly at constant speeds; dynamic speed variations are not considered at this stage. This assumption simplifies the calculation of flight time and operational cost but may affect cost estimation and route-feasibility evaluation in real post-disaster environments, where UAV speed and endurance can be influenced by wind, payload variation, battery state, altitude, route geometry, and weather. Variable speed and payload-dependent endurance will be considered in future work.
5. When the MUAV and a SUAV rendezvous at a predetermined meeting point, the party arriving first enters a waiting state (incurring no additional cost) until the other arrives, after which the handover of communication equipment (for replenishment or retrieval) is completed.

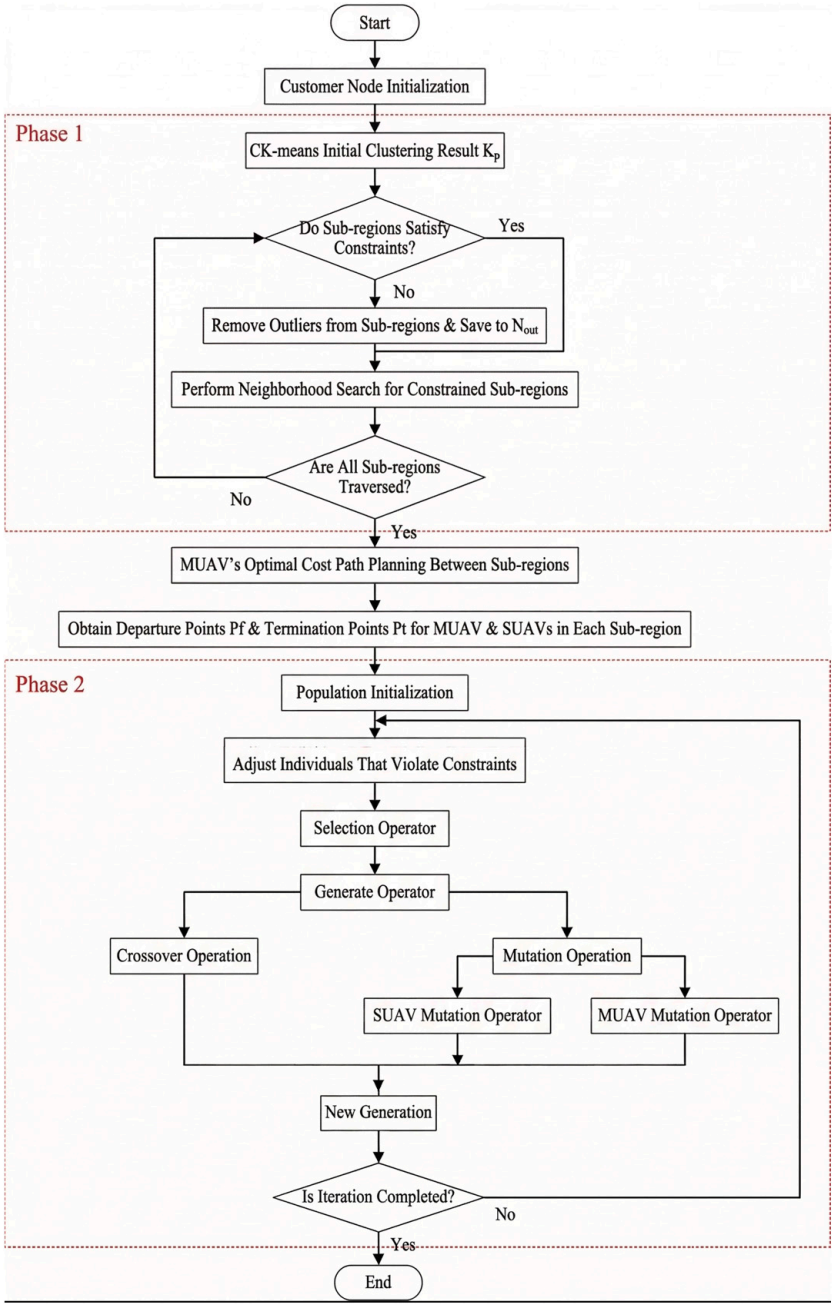

Figure 1. Two-phase solution algorithm flowchart.

2.1. Modeling of a Heterogeneous Unmanned Platform Emergency System with Mission Timeliness Constraints

In this paper, the heterogeneous platform coordinated scheduling optimization problem is decomposed into two subproblems: MUAV path planning and SUAV path planning. As the MUAV's payload constraint is introduced, its path planning between sub-regions must not only consider flight distance but also satisfy real-time capacity limitations.

The parameters and their meanings are defined in Table 1.

Table 1. Symbols and descriptions of system.

Parameter	Description
N	The total number of points requiring deployment or redeployment of communication equipment
P	Set of the total number of points requiring deployment of communication equipment $P = \{p_1, p_2, \ldots, p_N\}$
A	Set of SUAVs, $A = \{a_1, a_2, \ldots, a_n\}$
K	Subset of deployment point regions, $K = \{k_1, k_2, \ldots, k_n\}$, k_i represents the i-th sub-region
C	Set of cluster centers, $C = \{c_1, c_2, \ldots, c_n\}$, c_i represents the cluster center of the i-th sub-region
N_k	Number of deployment point sub-regions
N_s	Number of deployment points with deployment demands
P_s	Set of deployment points with deployment demands, $P_s = \{p_1, p_2, \ldots, p_{N1}\}$
N_q	Number of retrieval points of communication equipment
P_q	Set of deployment points with deployment requirements, $P_q = \{p_1, p_2, \ldots, p_{N2}\}$
N_{sq}	Number of deployment points with either deployment or redeployment
P_{sq}	Set of deployment points with either deployment or redeployment, $P_{sq} = \{p_1, p_2, \ldots, p_{N3}\}$, satisfying $P_{sq} = P_s \cap P_q$
P_w	Set of deployment points with no demand status, $P_w = P - P_s \cup P_q$
P_f	Takeoff point for the SUAV swarm within the region
P_l	Landing point for the SUAV swarm within the region
v_a	SUAV flight speed
v_t	MUAV flight speed
P_a	Set of points traversed by SUAVs within a sub-region, $P_a = P_f \cup P_s \cup P_l$
P_t	Set of points traversed by the MUAV within a sub-region, $P_t = P_f \cup P_q \cup P_l$
P_{total}	Set of all points, $P_{total} = P_f \cup P \cup P_l$
e	Maximum allowed deployment time for the MUAV or SUAV at a deployment point
s_p	Penalty cost per unit time when the MUAV or SUAV exceeds the maximum deployment time
τ_c	Actual deployment time of the MUAV or SUAV at deployment point p_c

2.2. SUAV Deployment Task Model for Communication Equipment Under Mission Timeliness and Payload Constraints

The parameters and meanings of the SUAV are shown in Table 2:

Table 2. SUAV parameters and descriptions.

Parameter	Meaning
S_A	Total flight cost of the SUAV swarm within the region
S_A^k	Total flight cost of the SUAV swarm within region k
S_a^K	Total flight distance of the a-th SUAV within the area
S_a^k	Flight cost of the a-th SUAV within region k
$S_{a(p_i,p_j)}^k$	Flight cost of the a-th SUAV from point p_i to point p_j in region k
$D_{a(p_i,p_j)}^k$	Distance traveled by the a-th SUAV from point p_i to p_j in sub-region k
$D_{\max}^a$	Ideal maximum flight range of the a-th SUAV

Table 2. *Cont.*

Parameter	Meaning
$D_{\max}$	Maximum flight distance under ideal maximum payload capacity and energy consumption of the SUAV
s_d	Flight cost per unit time for the SUAV
s^a_{fix}	Fixed dispatch cost for the SUAV
Q^k_a	Actual payload capacity of the a-th SUAV at takeoff in sub-region k
$Q^a_{\max}$	Ideal maximum payload capacity of the a-th SUAV
d^k_i	Weight of the communication device to be delivered to the i-th deployment point with deployment demand in sub-region k
N^k_s	Number of deployment points with deployment demand in region k

The SUAV deployment subproblem aims to minimize the operational cost of the SUAV swarm within each sub-region. The objective function consists of three components: the fixed SUAV dispatch cost, the SUAV flight cost, and the penalty cost caused by exceeding the mission time window. Based on the parameters and decision variables defined above, the SUAV deployment subproblem is formulated in the following standard optimization form:

$$\min S_A = \sum_{k\in K} S^k_A \tag{1}$$

$$\begin{aligned} D^k_a &= \textstyle\sum_{(p_i,p_j)\in p_a, i\neq j} D^k_{a(p_i,p_j)} \\ \text{s.t. } D^k_a &\le D^a_{\max} \\ D^a_{\max} &= \frac{Q_{\max}}{Q_{a(p_f)}} \times D_{\max} \end{aligned} \tag{2}$$

$$Q^k_a \le Q^a_{\max} \tag{3}$$

$$d^k_i \le Q^a_{\max} \tag{4}$$

$$\sum_{a\in A} X^k_a \le |A| \tag{5}$$

$$\sum_{i\in p_s} d^k_i = \sum_{a\in A} Q^k_a \le \sum_{a\in A} Q^a_{\max} \tag{6}$$

$$\textstyle\sum_{a\in A} \sum_{p_i\in P_s, i\neq j} X^k_{a(p_i,p_j)} = 1 \tag{7}$$

$$\textstyle\sum_{a\in A} \sum_{p_i\in P_s, i\neq j} \sum_{p_j\in P_s, i\neq j} X^k_{a(p_i,p_j)} = N^k_s \tag{8}$$

Among them, (1) is the objective function; constraint condition (2) indicates that the actual flight distance of the SUAV does not exceed its maximum flight distance; constraint condition (3) states that the actual payload capacity of the a-th SUAV cannot exceed the SUAV's maximum payload capacity; constraint (4) specifies that the weight of a single communication device must not exceed the ideal maximum payload capacity of each SUAV; in order to minimize the number of round trips and thus reduce the total flight distance, constraint condition (5) stipulates that each SUAV can take off at most once within one region; constraint condition (6) indicates that the total weight of communication devices in that region must not exceed the combined maximum payload capacity of all SUAVs; and (7) and (8) ensure that all deployment points with deployment demands are served by SUAVs exactly once where the binary domains are $X^k_a \in \{0,1\}$ and $X^k_{a(p_i,p_j)} \in \{0,1\}$, for all $a \in A, k \in K$, and $p_i, p_j \in P_k$.

2.3. Modeling for MUAV Path Planning in Communication Equipment Deployment Under Payload Constraints

MUAV parameters and descriptions are shown in Table 3:

Table 3. MUAV parameters and descriptions.

Parameter	Description
S_T	Total flight cost of the MUAV
S_i^k	Total flight cost of the MUAV within sub-region k
S_o	Total flight cost of the MUAV between sub-regions
s_c	Flight cost per unit time for the MUAV
$S_{i(p_i,p_j)}^k$	Flight cost for the MUAV from retrieval-demand deployment point p_i to retrieval-demand deployment point p_j within sub-region k
$S_o^{(k_i,k_j)}$	Flight cost for the MUAV from sub-region K_i to sub-region K_j
$Q_{\max}^t$	Ideal maximum load capacity of the MUAV
Q_k^t	Total load of the MUAV before arriving at the k-th sub-region
Q_q^k	Weight of communication devices to be picked up by the MUAV in the k-th sub-region
b_i^k	Weight of the communication device to be picked up from the i-th deployment with retrieval demand in sub-region k
$D_{i(p_i,p_j)}^k$	Distance traveled by the MUAV from deployment point p_i to p_j (both with retrieval demand) in sub-region k
N_t^k	Number of customers with retrieval demand in sub-region k
$D_o^{(k_i,k_j)}$	Distance traveled by the MUAV from sub-region K_i to sub-region K_j
D	Total flight distance of all unmanned vehicles in the collaborative deployment and retrieval system
S	Total flight cost of all unmanned vehicles in the collaborative deployment and retrieval system

The binary decision variables used in the SUAV and MUAV routing models are listed separately in Table 4.

Table 4. Decision variables used in the model.

Variable	Description
X_a^k	binary variable that equals 1 if SUAV a is dispatched in sub-region k; otherwise 0
$X_{a(p_i,p_j)}^k$	binary variable that equals 1 if SUAV a travels from node p_i to p_j in sub-region k; otherwise 0
$X_{i(p_i,p_j)}^k$	binary variable that equals 1 if MUAV travels from p_i to p_j in sub-region k; otherwise 0
$X_{o(k_i,k_j)}$	binary variable that equals 1 if MUAV moves from sub-region k_i to k_j; otherwise 0

The MUAV routing subproblem determines both the intra-region retrieval route and the inter-region visiting sequence of the MUAV. The objective function includes the MUAV flight cost within sub-regions, the MUAV flight cost between sub-regions, and the penalty cost associated with delayed deployment. Based on the parameters and decision variables defined above, the MUAV routing subproblem is formulated in the following standard optimization form:

$$\min S_T = \sum_{k\in K}\sum_{(p_i,p_j)\in p_t, i\neq j} S_{i(p_i,p_j)}^k X_{i(p_i,p_j)}^k + S_o^{(k_i,k_j)} X_{o(k_i,k_j)} + s_p\left(\tau_j - eX_{i(p_i,p_j)}^k\right)^+ \quad (9)$$

$$\text{s.t. } 0 \le \sum_{k\in K}\sum_{a\in A} Q_a^k \le Q_{\max}^t \quad (10)$$

$$0 \le Q_k^t \le Q_{\max}^t \tag{11}$$

$$0 \le Q_k^t + \sum_{a \in A} Q_a^k - Q_q^k \le Q_{\max} \tag{12}$$

$$b_i^k \le Q_{\max}^t \tag{13}$$

$$\sum_{k \in K} \sum_{i \in P_q} b_i^k \le Q_{\max}^t \tag{14}$$

$$\sum_{p_i \in P_q, i \ne j} X_{it(p_i,p_j)}^k = 1 \tag{15}$$

$$\sum_{p_i \in P_q, i \ne j} \sum_{p_j \in P_q, i \ne j} X_{it(p_i,p_j)}^k = N_t^k \tag{16}$$

$$\sum_{k_i \in K, i \ne j} X_{o(k_i,k_j)} = 1 \tag{17}$$

$$\sum_{k_j \in K} \sum_{k_i \in K, i \ne j} X_{o(k_i,k_j)} = N_k \tag{18}$$

Among them, (9) is the objective function; (10) indicates that the total weight of communication devices to be delivered within the entire deployment area does not exceed the MUAV's ideal maximum payload capacity; (11) states that before serving the k-th sub-region, the MUAV's load does not exceed its ideal maximum payload capacity; (12) ensures that after completing the deployment and retrieval tasks in each sub-region, the load inside the MUAV will not exceed its ideal maximum payload capacity; (13) specifies that the weight of a single communication device to be picked up cannot exceed the MUAV's ideal maximum payload capacity; (14) states that the total weight of communication devices to be picked up in the entire task area must not exceed the MUAV's ideal maximum payload capacity; and constraints (15) and (16) ensure that each retrieval point is served exactly once by the MUAV, while constraints (17) and (18) jointly ensure that each sub-region is visited exactly once by the MUAV. where the binary domains are $X_{i(p_i,p_j)}^k \in \{0,1\}$ and $X_{o(k_i,k_j)} \in \{0,1\}$.

Finally, the overall objective function integrates the SUAV-related cost and the MUAV-related cost. The total system cost is minimized as follows:

$$\min S = S_A + S_T \tag{19}$$

From an engineering perspective, the objective functions evaluate both flight distance and the operational cost of heterogeneous MUAV–SUAV cooperation. The time-window penalty reflects the additional loss caused by delayed communication-device deployment, while the deployment–retrieval payload balance ensures that the MUAV has sufficient capacity for both newly deployed and retrieved devices. Therefore, payload constraints are directly related to route feasibility, since a shorter route may still be infeasible if the MUAV or SUAV payload limit is violated. In addition, the rendezvous waiting condition is treated as an operational assumption without introducing additional waiting cost in the present model.

Remark: This paper extends the Time-dependent Collaborative SUAV Path Planning Problem (TDCDPPP) proposed in reference [25] by further introducing the payload constraint of the MUAV and the mission timeliness constraint for sub-regions. The inclusion of these two types of constraints increases the complexity of the problem and enhances its alignment with real-world scenarios. The payload constraint not only limits the total amount of communication equipment the MUAV can carry in a single trip but also, by influencing the total equipment allocation between the MUAV and UAVs within each sub-region, inversely determines the feasibility of the initial sub-region division in the first stage. Meanwhile, the mission timeliness constraint requires all equipment to be

deployed within specified time windows, imposing stricter timing requirements on the coordinated path planning of the MUAV and UAVs. These constraints render the Heterogeneous Collaborative Optimization Algorithm (HDFOS) from reference [25] unable to directly solve the new problem. Therefore, this paper proposes improvements in a two-stage algorithm: First, a new clustering algorithm is introduced to generate an initial sub-region division that satisfies both payload and timeliness constraints. Second, in the path optimization stage, the strategy of separately solving the paths for the MUAV and UAVs, as used in the original algorithm, is abandoned. Instead, a unified encoding scheme and an integrated mutation operator are designed, merging the path planning for the heterogeneous platforms into a single IAGA framework for simultaneous optimization. Through carefully designed genetic operators and adaptive mechanisms, this algorithm achieves a higher-quality coordinated scheduling solution while effectively controlling computational complexity.

3. Optimal Cost Path Planning Algorithm Design

This section develops a path planning algorithm to minimize the cost of collaborative deployment and retrieval of communication devices by multiple MUAVs and SUAVs, as described earlier. Due to the differing roles of MUAVs and SUAVs, we continue to use a two-stage approach that first clusters the target locations and then solves the path planning problem. The basic steps of the algorithm are as follows: first, deployment points are divided into several sub-regions that satisfy constraints (2–4, 6, 11–13); then, the optimal path for MUAV between sub-regions is solved. Here, since only the flight between sub-regions by MUAV is considered, only path cost is involved. The MUAV inter-region visiting sequence can be abstracted as a TSP subproblem, because only the visiting order and path cost between sub-regions are considered at this stage.

The algorithm framework is shown as follows:

3.1. Clustering Algorithm Design

Due to the addition of MUAV payload capacity constraints in this paper, clustering must comprehensively consider the total weight of communication devices delivered by SUAVs (i.e., satisfying constraints (2–4) and (6)) and the weight of communication devices retrieved by MUAV (i.e., satisfying constraints (11–13)). To avoid a situation in any sub-region where the total weight of communication devices to be delivered is less than the total weight of communication devices to be retrieved, which would lead to exceeding the MUAV's payload capacity constraint, this paper must ensure that after clustering, the total weight of communication devices to be deployed in each sub-region is not less than the total weight of communication devices to be retrieved. The increase in constraint conditions and the heightened coupling between MUAVs and SUAVs make the clustering problem significantly more complex, rendering the clustering method proposed in [25] inadequate. Following this line of thinking, this subsection improves upon the Ck-means algorithm by adding neighborhood search to the original algorithm, designing a K-means clustering algorithm based on neighborhood search.

Objective function

$$J(K) = \min \sum_{j=1}^{n_k} \sum_{p_i \in k_j} \left|\left| p_i - \mu_{(j)} \right|\right|_2^2. \tag{20}$$

$$\forall (p_i \in k_i) \left|\left| p_i - \mu_{(j)} \right|\right|_2 \leq D_{\max}^a \tag{21}$$

$$0 \leq \sum_{i \in p_q} b_i^k \leq Q_{\max}^t \tag{22}$$

$$0 \leq \sum_{j \in p_s} d_j^k \leq \sum_{a \in A} Q_{\max}^a \tag{23}$$

$$\sum_{i \in p_q} b_i^k \leq \sum_{j \in p_s} d_j^k \tag{24}$$

$$\forall (k \in K)(\sum_{i \in p_q} b_i^k + \sum_{j \in p_s} d_j^k) > 0 \tag{25}$$

Among them, (20) is the objective function for clustering; (21) indicates that the distance between any deployment point with deployment demand within a sub-region and its cluster center does not exceed the maximum flight range of the SUAV; (22) states that the total demand of deployment points requiring retrieval deployment in sub-region k does not exceed the MUAV's maximum load capacity; (23) states that the total demand of deployment points requiring deployment in the k-th sub-region does not exceed the combined maximum payload capacity of all SUAVs; (24) states that the total demand for deployment within sub-region k is not less than the total demand for retrieval; (25) ensures that no sub-region consists solely of deployment points with no demand.

Specific clustering steps are as follows:

(a) Cluster the deployment points using the CK-means algorithm to obtain an initial clustering result. Since the state of each deployment point is determined by its deployment quantity and retrieval quantity, any deployment point p_i can be uniquely represented by a two-dimensional array, that is $p_i(w_{si}, w_{qi})$, where w_{si} and w_{qi} denote the deployment quantity and retrieval quantity of deployment point p_i, respectively. It should be noted that the clustering result at this stage already satisfies the payload capacity and range constraints of the SUAVs. Therefore, it is only necessary to further adjust the clustering to meet the MUAV's payload capacity constraint. As the MUAV has no range limitation, the process essentially involves reassigning those deployment points that only require retrieval service, represented as $p_i(0, w_{qi})$, which do not satisfy the requirements within the current clusters.

(b) Calculate the distances from each cluster center to all others, obtaining a distance matrix between the cluster centers.

(c) Calculate the deployment volume $\sum_{j \in p_s} d_j^k$ and the retrieval volume $\sum_{i \in p_q} b_i^k$ within each sub-region to obtain a set of sub-regions that satisfy constraint (24) (valid) and a set of sub-regions that do not satisfy constraint (24).

(d) Process each sub-region within the set. First, calculate the distances from all deployment points satisfying $p_i(0, w_{qi})$ to the cluster center within each sub-region. Then sort these distances in descending order.

(e) For each illegal sub-region, sequentially strip away deployment points that satisfy $p_i(0, w_{qi})$ until the sub-region becomes legal. The stripped deployment points are collectively referred to as noise points.

(f) Legitimate sub-regions perform a neighborhood search around their cluster centers. Under the premise of satisfying constraint (24), noise points near the cluster center are incorporated into the sub-region. This process continues until all noise points have been assigned, completing the regional division.

The pseudocode is provided in Algorithm 1.

Algorithm 1: K-means-NS Pseudocode

Input: The weight demand of the communication devices to be deployed for the i-th deployment d_i; the weight demand of the communication device to be retrieved for the i-th deployment b_i; the ideal maximum payload capacity of the a-th SUAV $Q^a_{\max}$; the expected maximum load capacity of the MUAV $Q^t_{\max}$; the set of subregions obtained via the CK-means algorithm $K_p = \left\{k_p^1, k_p^2, \ldots, k_p^n\right\}$

$Iter = 1$ (Iter is the iteration count)
While $Iter \le size(K_p)$
If within subregion k_p^{iter}: $\sum_{i \in p_q} b_i^k > Q^t_{\max}$ || $\sum_{i \in p_q} b_i^k > \sum_{j \in p_s} d_j^k$
$D \leftarrow$Calculate the distance from each point to all cluster centers
While $\sum_{i \in p_q} b_i^k > Q^t_{\max}$ || $\sum_{i \in p_q} b_i^k > \sum_{j \in p_s} d_j^k$
$N_{oi} \leftarrow$ Remove the farthest point $p_i(0, w_{qi})$ from subregion k_p^{iter} and store it in the noise point set N_{oi}
$k_p^{iter} \leftarrow$ Update deployment points within the subregion
End while
Else continue
End if
$Iter = Iter + 1$
End while
$Iter0 = 1$
$Iter = 1$
While $Iter0 \le size(N_{oi})$
While $Iter \le size(K_p)$
If adding the noise point to subregion k_p^{iter} satisfies the constraints

$$\sum_{i \in p_q} b_i^k \le Q^t_{\max} \;\&\&\; \sum_{i \in p_q} b_i^k \le \sum_{j \in p_s} d_j^k$$

$k_p^{iter} \leftarrow N_{oi}(Iter0)$
End if
$Iter = Iter + 1$
End while
$Iter0 = Iter0 + 1$
End while

Output : The set of subregions $K_p, K_p = \left\{k_p^1, k_p^2, \ldots, k_p^n\right\}$; the set of cluster centers C, $C = \{c_1, c_2, \ldots, c_n\}$; the set of noise points N_{oi}

Note: Not all noise points in N_{oi} can be assigned to feasible sub-regions after neighborhood search. If a noise point cannot be inserted into any sub-region without violating constraint (24), it is temporarily kept outside the sub-region set rather than being forced into an infeasible cluster. Since the MUAV is not subject to the SUAV range constraint, these unassigned noise points are subsequently treated as independent MUAV service points and are considered together with the cluster centers during the MUAV inter-sub-region route planning. The MUAV route is then solved under the premise of satisfying the MUAV payload constraint.

3.2. Design of a Coordinated Deployment Path Planning Algorithm for Heterogeneous Platforms Within Sub-Regions

First, the traversal order between sub-regions is solved using the ant colony algorithm. Then, within each sub-region, an IAGA is designed to solve the path planning problem for MUAVs and SUAVs with the minimum cost. The SUAV intra-region routing subproblem is related to the 2p-mVRPTW class because it involves multiple SUAVs, pickup-and-delivery operations, and mission time-window constraints. Therefore, this paper takes the minimum-cost path planning of the SUAV swarm within a sub-region as an example to illustrate the algorithm design in detail. The specific algorithm design is as follows:

1. Encoding method and initialization:

This paper still adopts the sequence encoding method, setting the population size to N_p. Each individual's gene consists of two parts, the routing sequence and the breakpoint sequence, and is initialized using prior knowledge. The individual gene is illustrated in Figure 2 below:

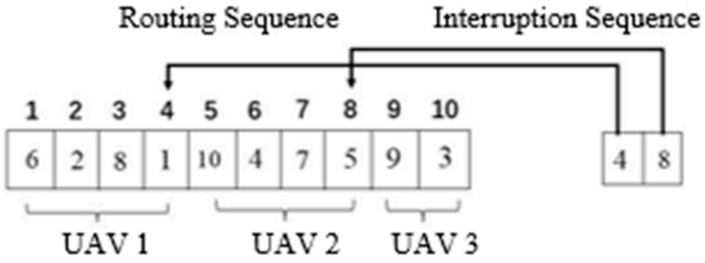

Figure 2. Schematic diagram of individual gene sequence encoding.

The 'Routes sequence' defines the overall task visiting order, and the 'Interruption sequence' separates the routes of individual SUAVs.

The launch point is the location of the deployment point within this region that has deployment or retrieval needs and is closest to the landing point of the previous sub-region (or the starting point where the warehouse is located). The endpoint is the cluster center point of the sub-region.

The hybrid encoding jointly represents the MUAV visiting sequence and the SUAV task assignment in one chromosome, which allows the fitness function to evaluate heterogeneous platform coordination directly. The feasibility flag is used to distinguish feasible and infeasible individuals after repair, so that infeasible solutions caused by payload or range violations can be retained with lower priority instead of being immediately discarded. Compared with a conventional adaptive GA, this design preserves population diversity while guiding the search toward feasible coordinated routes under the coupled MUAV–SUAV constraints.

2. Population Individual Adjustment

For individuals that do not satisfy the constraint conditions (2–4, 6), the adjustment strategy from [25] is still employed to modify them, aiming to make each individual feasible. However, due to the randomness inherent in the initial path permutation and the demand of each deployment point, a small number of individuals may still fail to meet the constraints even after adjustment. Therefore, in this paper, and considering the need for genetic diversity, such individuals are defined as infeasible solutions but are nonetheless retained within the population. To distinguish between feasible and infeasible solutions, the encoding of an individual's gene is adjusted as follows in this paper. It is stipulated that the first code of the individual's gene serves as a flag bit. If the flag bit is 0, the solution represented by that individual's gene is a feasible solution; if the flag bit is -1, it represents an infeasible solution.

3. Adaptive Configuration

Inspired by the adaptive setup in genetic manipulation in ref. [22], this paper dynamically adjusts the number of crossover offspring and mutation offspring within the iteration period. The adaptive formula is as follows:

$$N_{cr} = round[(N_p - \gamma) \cdot e^{(-\frac{N_{iter}}{N_g})}] \tag{26}$$

$$N_{mu} = N_p - \gamma - N_{cr} \tag{27}$$

Here, N_g denotes the total number of iterations, N_{iter} denotes the current iteration number, $round[\cdot]$ represents the rounding operation, N_{cr} is the number of offspring obtained through the crossover operator, γ is the number of offspring selected by the selection operator to enter the next generation, and N_{mu} is the number of offspring obtained through the mutation operator.

4. Selection Operator Design

First, an elitism approach is adopted to select N_e optimal feasible individuals to enter the next generation. Infeasible individuals, which typically violate payload or range constraints, are retained by relaxing these constraints during fitness evaluation. They are then evaluated for fitness in the same way as other feasible individuals, so that all individuals in the population can participate in selecting the remaining $\gamma - N_e$ individuals to enter the next generation through a roulette wheel selection method.

5. Reproduction Operator Design

The design of reproduction operators mainly includes the design of the crossover operator and the mutation operator.

(a) Crossover Operator Design

Two individuals are randomly selected as parents from within feasible solutions, between feasible and infeasible solutions, and within infeasible solutions, respectively, to perform crossover and generate offspring, aiming to achieve global optimization of the algorithm. The specific operation is as follows:

A conventional crossover algorithm randomly selects a segment of the parents for crossover, generating two offspring. This approach results in low utilization of parental genes and low crossover efficiency. Therefore, to fully utilize the genes of each parent pair, this paper employs a method where a pair of genomes, each with a gene count of n_g, are crossed over group by group, with each group consisting of n_c genes. This generates a set of offspring numbering $n_g - n_c$, from which the best individual is selected as the offspring. Taking $n_c = 4$ as an example, the specific operation is illustrated in the following Figure 3:

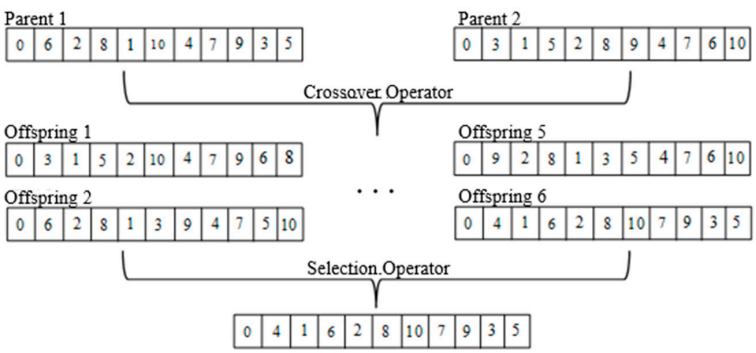

Figure 3. Selection crossover operator operation diagram. The ellipsis indicates intermediate offspring generated by the crossover operator that are omitted for clarity.

(b) Mutation Operator Design

(i) For the optimal cost path planning problem for MUAVs, the mutation operator in this paper adopts a commonly used multi-point mutation method. This involves randomly selecting a parent and rearranging chromosomes from multiple parent individuals to generate new offspring.

(ii) For the optimal cost path planning problem involving multiple UAVs, considering that the selection of mutation individuals in existing mutation operators is random and cannot evolve in a specific direction to find better solutions, this paper treats the path segment of each UAV as an operator. By altering the path of each UAV to achieve optimal individual cost, the overall optimal cost for the UAV swarm is ultimately realized. However, considering the high time complexity of mutating the gene segments of all UAV individuals, inspired by the pheromone setting in ant colony optimization algorithms, this paper uses the change in fitness value of each UAV in the parent individual as a reference for selecting each UAV's path segment in the next iteration. The roulette wheel algorithm is employed to select only one UAV's path segment for rearrangement in each iteration. Consequently, a larger change in the fitness value of a UAV's path segment indicates greater room for improvement, and thus a higher probability of being selected in the next iteration, allowing the parent individual to exhibit a trend of evolution towards optimizing the objective function. This operator thereby serves the algorithm's function of local search.

The pseudo code is provided in Algorithm 2:

Algorithm 2: IAGA pseudo code.

Input : Sub-region set $K_p, K_p = \left\{k_p^1, k_p^2, \ldots, k_p^n\right\}$; Cluster center set $C, C = \{c_1, c_2, \ldots, c_n\}$; Number of SUAVs Na; Population size N_p; Number of iterations x; Noise point N_{oi}

P_{fp} ←Calculate the deployment point in the next sub-region that is closest to the previous sub-region1.
C ←The cluster center set C serves as the destination
$Iter0 = 1$ ($Iter0$ is the iteration count)
While $Iter0 \leq Sizeof(K_p)$
    R, Dr Initialize the population to obtain path genes R and interrupted genes Dr
    $Iter1 = 1$
    While $Iter1 \leq x$
        $i = 1$
        While $i \leq N_p$
            If R_i, Dr_i Constraints are not met
            R_i, Dr_i←Adjust the path genes and interrupted genes of individuals that do not meet the constraints
            End if
            $Fit(i)$ ← Calculate the fitness value for each individual
            k_p^i ← Assign labels to the deployment points in each subregion
    End while
    ### Design of Selection Operator ###
    N_e ← Select the optimal individual N_e through elitism
    $R,\ Dr$ ← Select $\gamma - N_e$ individuals as offspring using the roulette wheel method
Design of Crossover Operator

Algorithm 2: Cont.

$Iter2 = 1$
For $Iter2 = 1 : N_{cr}$
$N_{off} \leftarrow$ Two individuals are selected as parents to generate offspring
$R, Dr \leftarrow$ Select the optimal individual from the offspring populationN_{off}
End for
Design of Mutation Operator
$Iter3 = 1$
If MUAV route genes
For $Iter3 = 1 : N_{mu}$
$R, Dr \leftarrow$ Parent individuals
End for
Else if SUAV path genes
For $Iter3 = 1 : N_{mu}$
$R_{mu}, Dr_{mu} \leftarrow$ Parent individuals
$Iter4 = 1$
For $Iter3 = 1 : y$
$R_{mu}, Dr_{mu} \leftarrow$Mutation of parent genes
End for
$R, Dr \leftarrow R_{mu}, Dr_{mu}$
End for
End if
End while
The optimal cost Dr and route planning R for the MUAV and multiple SUAVs in the region
End while

Output : the optimal cost Dr_z and the route planning sequence R_z for the MUAV and multiple SUAVs performing deployment and retrieval tasks within the region.

From the design of the adaptive function, as the number of iterations increases, the number of offspring generated by the crossover operator decreases, while the number generated by the mutation operator increases. This achieves a shift in the entire algorithm from global to local optimization, which will effectively address the shortcomings of traditional genetic algorithms, such as poor local search capability and slow convergence speed. The computational complexity of IAGA depends on the population size, the maximum number of generations, the chromosome length, and the fitness-evaluation procedure; therefore, the original linear-complexity statement has been removed.

It should be noted that the proposed IAGA is a heuristic algorithm and therefore does not provide a theoretical guarantee of global optimality. Nevertheless, its convergence behavior and solution quality are supported by several algorithmic mechanisms. First, the elitist selection strategy preserves the best feasible individuals found so far, preventing the current best solution from being lost during iteration. Second, the adaptive crossover and mutation mechanism balances global exploration and local exploitation by emphasizing crossover in the early stage and mutation-based refinement in the later stage. Third, infeasible individuals are retained with a feasibility flag, which helps maintain population diversity while guiding the search toward feasible solutions. Therefore, although the optimality gap cannot be theoretically guaranteed, the convergence curves and multi-scale numerical experiments in Section 4 empirically demonstrate that IAGA achieves stable convergence and improved solution quality compared with the benchmark algorithms.

Further theoretical analysis of optimality gaps and convergence bounds will be considered in future work.

4. Numerical Experiments and Analysis

The objective of this section is to validate the effectiveness of the proposed algorithm in solving the optimal cost problem for the sub-mother UAV swarm collaborative deployment system through numerical simulation experiments. First, the effectiveness of the designed K-means-NS algorithm is verified. Then, the performance of IAGA is evaluated by comparing it with other algorithms. Finally, the solution to the problem proposed in this paper using IAGA is provided.

The collaborative deployment and retrieval system still consists of 4 SUAVs and 1 MUAV. The SUAV parameters are set according to a representative urban cargo SUAV, with a maximum payload capacity of 10 kg per SUAV. The MUAV maximum payload capacity is set to 250 kg. For the cost settings, the MUAV flight cost per unit time is set to 24.72 CNY/h, the SUAV flight cost per unit time is set to 9.12 CNY/h, and the fixed dispatch cost per SUAV is set to 1 CNY/h.

The average flight speed of the SUAVs is 30 km/h, with a full-load endurance of 20 km. The MUAV's average flight speed is 20 km/h. When the deployment time of the MUAV or SUAV at a deployment node exceeds the allowed limit, the unit penalty cost is 1000 CNY/h.

The selected area sizes represent small-, medium-, and relatively large-scale emergency communication restoration tasks. The UAV payload, endurance, flight-speed, and cost parameters are set according to practical UAV specifications and relevant references, so that the numerical scenarios reflect typical heterogeneous MUAV–SUAV deployment conditions while maintaining controllable benchmark complexity.

It should be noted that the numerical experiments in this study are mainly based on randomly generated instances with limited problem scales. The current experimental design is intended to provide preliminary validation of the feasibility and comparative performance of the proposed framework under different scenario sizes, rather than exhaustive benchmark testing. A more robust experimental design, including multiple random seeds, larger-scale instances, averaged performance results, standard deviations, and computational time, will be conducted in future work to further evaluate the generalizability and stability of the proposed method.

4.1. Validation of the K-Means-NS Algorithm Effectiveness

Within a deployment area of 1.2 km $\times$ 1.2 km, 60 deployment points were randomly generated. Among these, 50 points are deployment points requiring deployment from SUAVs and MUAVs respectively, while the remaining deployment points are set as non-demand points. The weight of communication devices for deployment and the weight for retrieval at each deployment point are randomly distributed between 1 and 5 kg. The clustering results of the Ck-means algorithm and the K-means-NS algorithm are shown in Figure 4:

The data comparison between the K-means-NS algorithm and the Ck-means algorithm is shown in Table 5:

Table 5. Comparison of clustering results.

Method	Sub-Region No.	Total Weight of Communication Devices for SUAV Deployment Within the Sub-Region (kg)	Total Weight of Communication Devices for MUAV Retrieval Within the Sub-Region (kg)	Distance from the Farthest Point to the Cluster Center in the Sub-Region (m)
Ck-means	Sub-region 1	14.7878	14.7368	1681.2
	Sub-region 2	36.8332	29.8978	3483.6
	Sub-region 3	35.6267	26.5275	3799.5
	Sub-region 4	29.8815	33.6092	2518.3
	Sub-region 5	17.2071	14.3733	2337.5
	Sub-region 6	34.6312	17.4401	2750
K-means-NS	Sub-region 1	31.4888	23.6704	4272
	Sub-region 2	37.1254	25.5733	3573.3
	Sub-region 3	39.2428	35.6641	3649.5
	Sub-region 4	37.3787	32.7626	3443
	Sub-region 5	23.7317	18.9144	3261.6

As can be seen from Algorithm 1, in sub-region 4 divided by the Ck-means algorithm, the total weight of communication devices for deployment is less than the total weight for MUAV retrieval. After re-dividing the sub-regions using the K-means-NS algorithm, all sub-regions satisfy constraints (21–25). Furthermore, the reassignment of noise points improves the feasibility of the sub-region division. Figure 4 and Table 5 demonstrate the effectiveness of the K-means-NS algorithm.

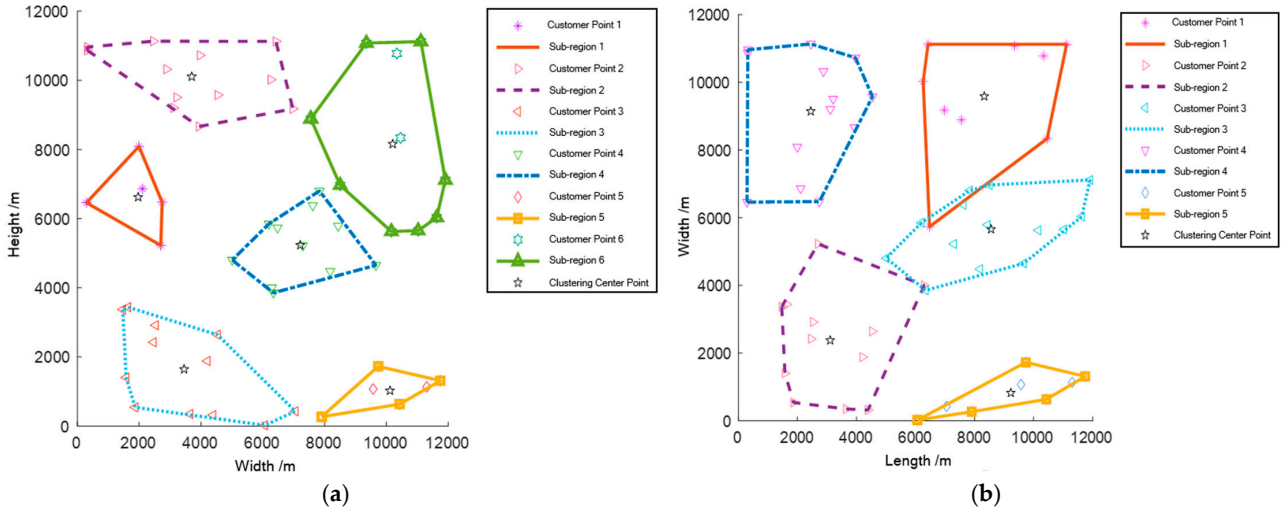

(**a**) (**b**)

Figure 4. Clustering results: (**a**) Ck-means clustering; (**b**) K-means-NS clustering. The coordinate axes are expressed in meters.

4.2. Effectiveness Analysis of IAGA

In this section, test cases are randomly generated for three different scales: a small-scale area (3 km × 3 km, with 15 deployment points each for deployment and retrieval demands), a medium-scale area (8 km × 8 km, with 30 deployment points each for deployment and retrieval demands), and a large-scale area (12 km × 12 km, with 60 deployment points each for deployment and retrieval demands). The optimal costs for these cases are solved respectively to validate the effectiveness of the algorithm proposed in this paper. The details are illustrated in Figure 5:

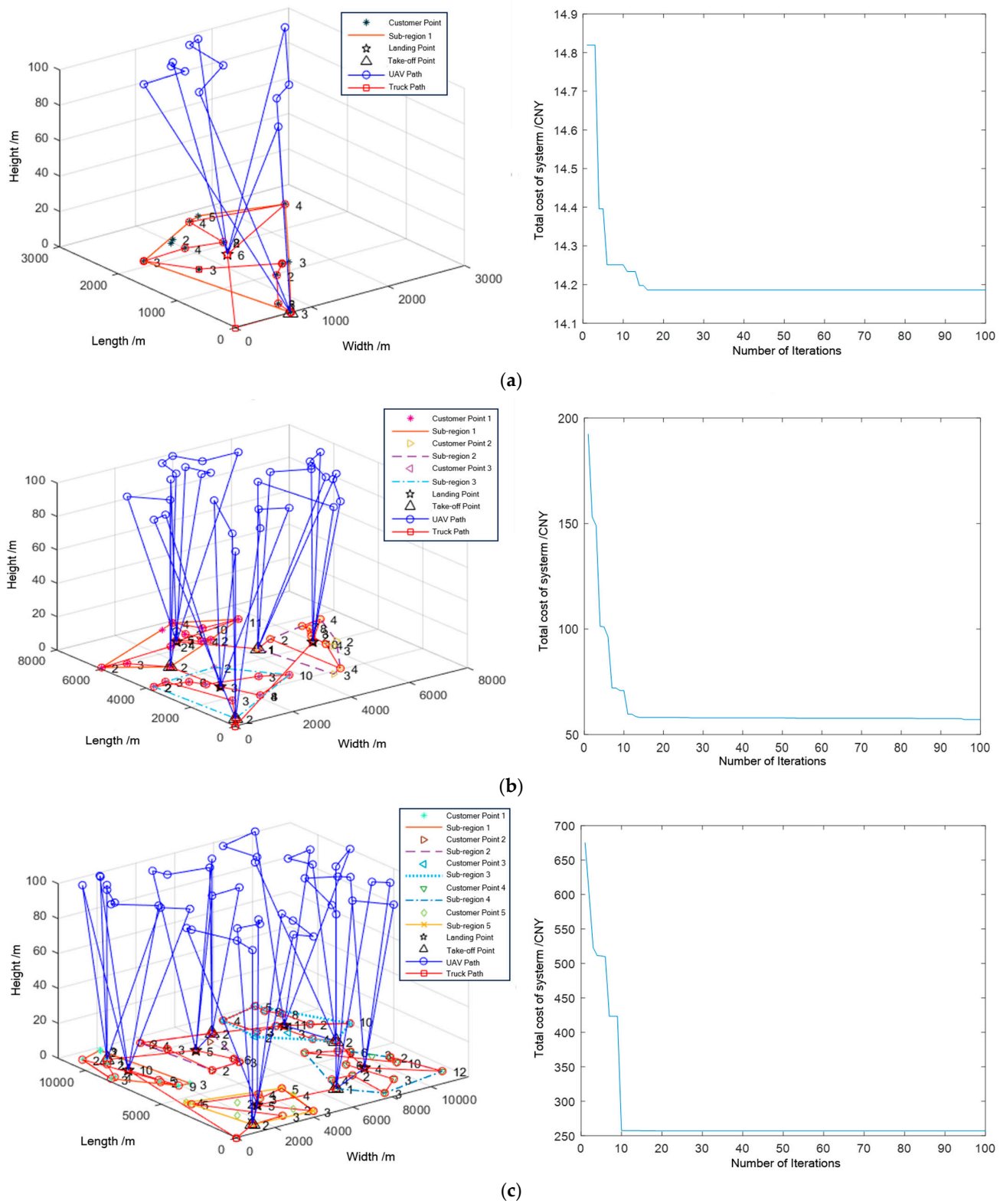

Figure 5. IAGA path planning results and iteration process: (**a**) Small area scenario (3 km × 3 km); (**b**) medium area scenario (8 km × 8 km); (**c**) large area scenario (12 km × 12 km).

As can be seen from Figure 5, the proposed algorithm effectively solves the optimal cost problem for the deployment and retrieval of communication devices by a sub-mother UAV swarm. This problem involves different mission time-window settings, and the algorithm successfully obtains the optimal costs under the constant-speed assumption. It is observed that in the randomly generated small-scale, medium-scale, and large-scale

deployment areas mentioned above, the optimal costs obtained by the algorithm are 14.1858CNY, 57.0703CNY, and 256.856CNY, respectively.

4.3. Performance Analysis of the Algorithm

In this section, the optimization capability and convergence speed of the proposed algorithm are evaluated through numerical simulations, and its performance in solving the sub-mother UAV swarm path planning problem within sub-regions is compared with that of the genetic algorithm (GA) and the G-PSHA mentioned in reference [25].

To assess the performance of IAGA, three scenarios with different scales are considered: a small-scale area (3 km × 3 km, with 12 deployment points each for deployment and retrieval demands), a medium-scale area (8 km × 8 km, with 30 deployment points each for deployment and retrieval demands), and a large-scale area (12 km × 12 km, with 45 deployment points each for deployment and retrieval demands). IAGA, GA, and G-PSHA are each run 10 times in this system, and the average values are taken. For a fair comparison, IAGA, GA, and G-PSHA are tested on the same randomly generated instances under the same population size, maximum number of iterations, stopping criterion, and computing environment. GA and G-PSHA follow their original crossover and mutation settings, whereas IAGA adopts the adaptive crossover–mutation mechanism described in Section 3.2. The results are as follows:

Figures 6–8 illustrate the optimization process across the three scenarios, while Tables 5–7 present the corresponding data for each scenario.

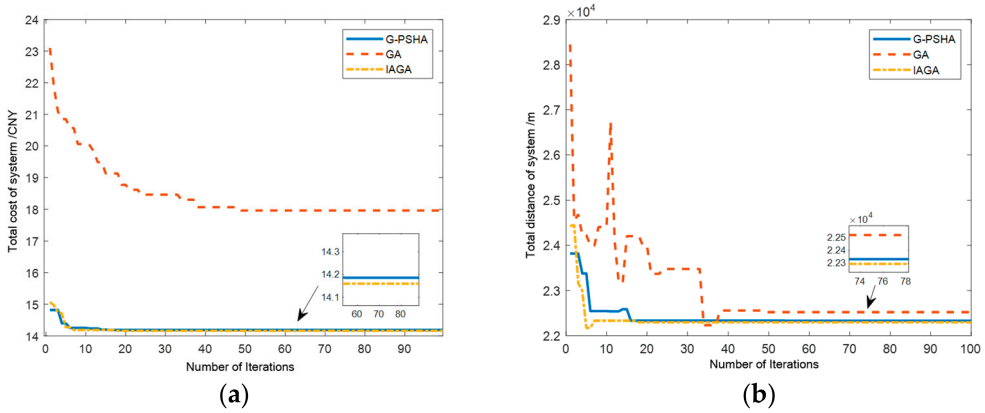

Figure 6. Small area scenario: (**a**) Comparison of total cost; (**b**) comparison of total distance.

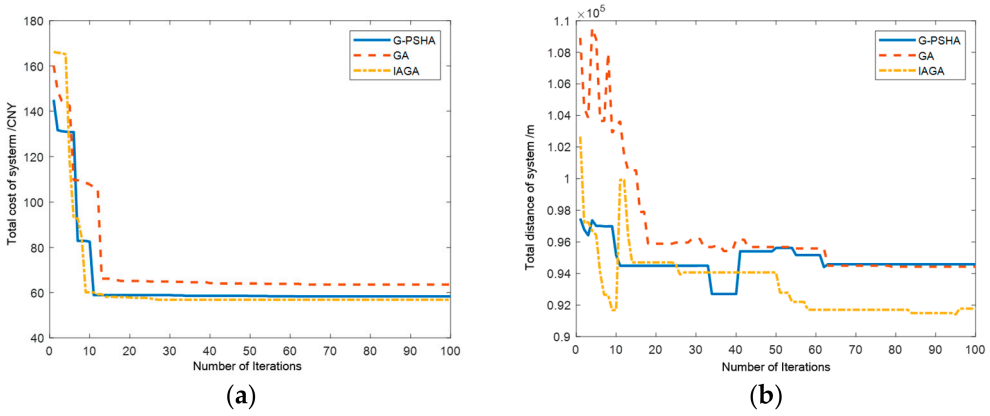

Figure 7. Medium area scenario: (**a**) Total cost comparison; (**b**) total distance comparison.

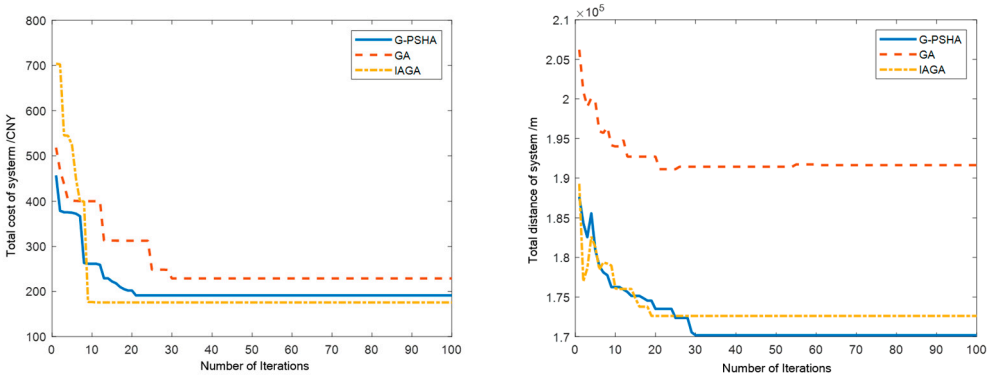

(**a**) (**b**)

Figure 8. Large area scenario: (**a**) Total cost comparison; (**b**) total distance comparison.

Table 6. Optimization results of different algorithms for small area scenarios.

Method	SUAV/MUAV No.	Flight Cost S_a^K/S_T/CNY	Total Flight Cost *S*/CNY	Total Flight Distance *D*/m
G-PSHA	SUAV 1	2.01	14.19	22,332
	SUAV 2	1.93		
	SUAV 3	1.98		
	SUAV 4	1.09		
	MUAV	7.16		
GA	SUAV 1	1.77	17.97	22,521
	SUAV 2	1.87		
	SUAV 3	3.09		
	SUAV 4	4.07		
	MUAV	7.17		
IAGA	SUAV 1	1.98	14.16	22,295
	SUAV 2	2.00		
	SUAV 3	1.92		
	SUAV 4	1.09		
	MUAV	7.15		

Table 7. Optimization results of different algorithms for medium area scenarios.

Method	SUAV/MUAV No.	Flight Cost S_a^K/S_T/CNY	Total Flight Cost *S*/CNY	Total Flight Distance *D*/m
G-PSHA	SUAV1	6.11	58.32	94,586
	SUAV2	7.09		
	SUAV3	7.18		
	SUAV4	1.93		
	MUAV	36.01		
GA	SUAV1	5.88	63.56	94,431
	SUAV2	2.21		
	SUAV3	7.46		
	SUAV4	12.27		
	MUAV	35.74		
IAGA	SUAV1	7.02	56.89	91,775
	SUAV2	3.61		
	SUAV3	7.18		
	SUAV4	4.33		
	MUAV	34.93		

Based on the numerical simulation results for the small-scale scenario, compared to GA, both IAGA and G-PSHA exhibit faster convergence, beginning to stabilize from the 7th and 6th iteration, respectively. This accelerated convergence is attributed to the introduction of the adaptive function, which promotes rapid convergence, and the enhancements made to the crossover and mutation operators, increasing the efficiency of each iteration. This demonstrates that the IAGA proposed in this paper effectively mitigates the slow convergence typically associated with traditional GA. Compared to the final result of 14.19 achieved by G-PSHA, IAGA obtains a result of 14.16, indicating stronger optimization capability. This validates the effectiveness of the genetic algorithm improvements proposed in this paper under small-scale conditions.

For the medium-scale scenario, Figure 7 compares the convergence behavior, total cost, and total flight distance of the three algorithms, while the detailed optimization results are summarized in Table 7, it can be observed that the convergence speeds of all three algorithms decrease. Specifically, G-PSHA shifts from starting to converge at the 6th iteration in the small-scale scenario to the 13th iteration in the medium-scale scenario, while IAGA shifts from the 7th iteration to the 9th iteration. Therefore, compared to G-PSHA, IAGA demonstrates stronger robustness in convergence speed. Meanwhile, by comparing the total costs, the solution obtained by IAGA is shown to be more optimal.

For the large-scale scenario, it can be observed that IAGA outperforms the other two algorithms in terms of both convergence speed and optimization capability. A comparison between the total cost and total distance further indicates that cost optimality and distance optimality are not necessarily consistent. Although G-PSHA obtains the shortest total distance, its total cost is not the lowest, because the objective function considers not only flight distance but also platform-dependent flight cost, SUAV activation cost, and time-window penalty cost. In particular, the MUAV and SUAVs have different unit flight costs, and dispatching more SUAVs may reduce local travel distance but simultaneously increase fixed activation costs. Conversely, allowing the SUAV swarm to travel a longer distance can still be economically preferable when it avoids excessive MUAV movement or reduces penalty costs caused by delayed deployment. This explains why, as shown in Table 8, the flight distance of the SUAV swarm can be longer than that of the MUAV while its operational cost remains significantly lower. Therefore, the proposed model does not simply pursue the shortest route; instead, it balances distance, heterogeneous platform cost, SUAV activation, and timeliness penalty to obtain a lower total deployment cost.

In addition, the improvement of IAGA mainly comes from the second-stage coordinated route optimization. The hybrid encoding enables the MUAV visiting sequence and SUAV task assignment to be optimized jointly, while the adaptive crossover–mutation mechanism and historical-improvement-based mutation operator enhance local search. These designs help reduce unnecessary SUAV dispatches, improve SUAV task allocation, and lower delayed-deployment penalties under the coupled payload and time-window constraints.

Figure 9 further compares the optimal system costs obtained with and without time-window constraints under the three deployment scales. The introduction of time-window constraints increases the total system cost because delayed arrivals generate additional penalty costs and restrict the range of feasible routing decisions. More importantly, the cost difference becomes more relevant as the task scale increases, since a larger number of deployment points makes it more difficult for the MUAV and SUAVs to complete all communication-device deployment tasks within the prescribed time limits. This result reveals a practical trade-off between deployment urgency and operational cost: stricter time requirements can accelerate emergency communication restoration but may require additional SUAV dispatches, more direct flight routes, or higher penalty expenditures.

Therefore, emergency decision-makers should jointly determine the allowable deployment time, available UAV resources, and acceptable operational cost according to the urgency of communication restoration. Future work will further examine the influence of other factors, such as penalty cost, the number of SUAVs, SUAV payload, MUAV payload, SUAV endurance, and communication-device weight.

Table 8. Optimization results of different algorithms for large area scenarios.

Methods	SUAV Number	Flight Cost S_a^K/S_T/CNY	Total Flight Cost *S*/CNY	Total Flight Distance *D*/m
G-PSHA	SUAV1	11.95	191.26	170,170
	SUAV2	11.37		
	SUAV3	10.35		
	SUAV4	0		
	MUAV	157.59		
GA	SUAV1	10.38	228.85	191,630
	SUAV2	0		
	SUAV3	11.96		
	SUAV4	17.79		
	MUAV	188.72		
IAGA	SUAV1	7.02	175.73	170,830
	SUAV2	3.61		
	SUAV3	7.18		
	SUAV4	4.33		
	MUAV	142.06		

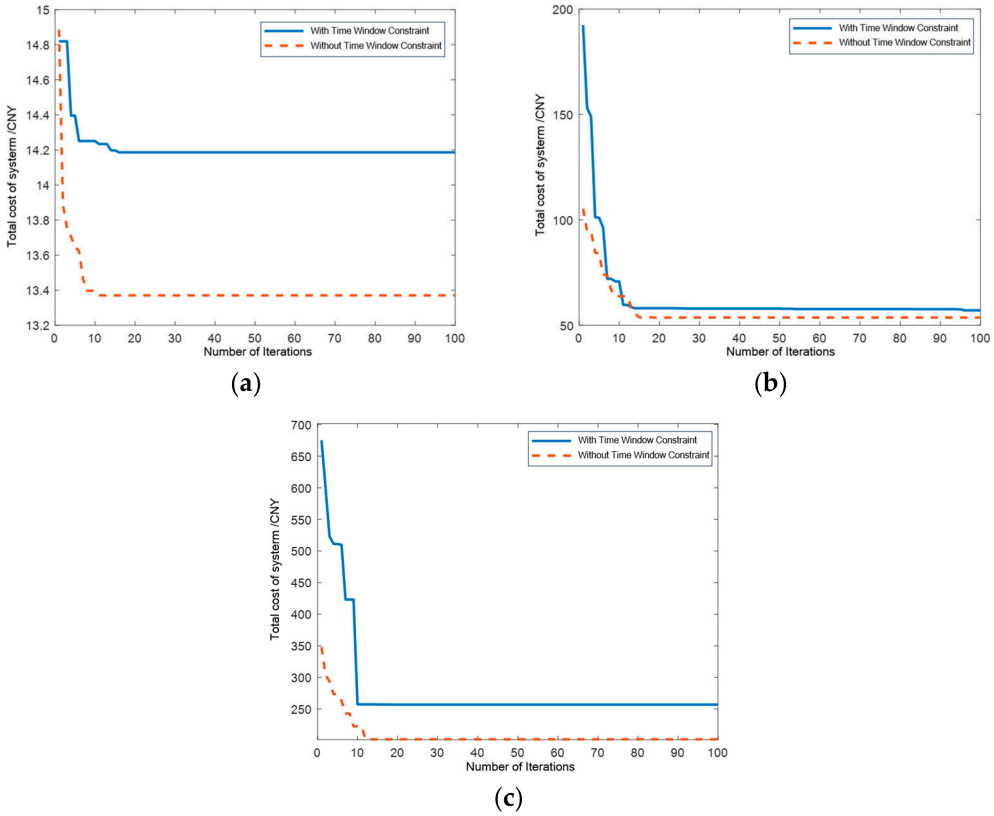

Figure 9. Optimal cost comparison between scenarios with and without time window constraints across different ranges: (**a**) Cost comparison with and without time windows in the small-scale area; (**b**) cost comparison with and without time windows in the medium-scale area; (**c**) cost comparison with and without time windows in the large-scale area.

Therefore, the improvement of IAGA over G-PSHA primarily stems from its enhanced local search capability (via the historical-improvement-based mutation) and its integrated optimization framework that better balances SUAV activation costs and time-window penalties under payload constraints.

5. Conclusions

This paper proposes a two-stage coordinated deployment and routing framework for a sub–mother UAV swarm in power-grid emergency communication scenarios. The K-means-NS algorithm generates feasible sub-regions while satisfying SUAV endurance and payload constraints and maintaining the deployment–retrieval payload balance, whereas the IAGA optimizes the coordinated routes of the MUAV and SUAVs under mission timeliness constraints. In the small-, medium-, and large-scale scenarios, IAGA reduces the total flight cost by approximately 21.2%, 10.5%, and 23.2% compared with GA and by approximately 0.2%, 2.5%, and 8.1% compared with G-PSHA, respectively, demonstrating its effectiveness across different problem scales. These findings suggest that the proposed framework can provide decision support for emergency communication restoration by balancing deployment urgency, UAV resource allocation, and total operating cost.

Nevertheless, the current model assumes constant UAV speeds, simplified energy consumption, and deterministic task information, and the numerical experiments are mainly based on randomly generated instances.

Future work will incorporate variable UAV speeds, payload-dependent energy consumption, uncertain mission conditions, communication-coverage constraints, and validation using real or realistic power-grid emergency data to further improve the practical applicability of the proposed framework.

Author Contributions: Conceptualization, Y.G., Y.S. and W.Y.; methodology, M.H., J.L. and W.Y.; software, S.Y.; validation, X.L., Y.Z. and J.L.; formal analysis, C.L.; investigation, Y.X. and Y.G.; resources, Y.S. and W.Y.; data curation, C.L., M.H. and Y.Z.; writing—original draft preparation, J.L.; writing—review and editing, Y.X.; visualization, Y.Z., W.Y. and S.Y.; supervision, W.Y.; project administration, W.Y.; funding acquisition, C.L. All authors have read and agreed to the published version of the manuscript.

Funding: This research was funded by the China Southern Power Grid Co., Ltd. Technology Project (No. GZKJXM20240598) and Liaoning Provincial Natural Science Foundation (General Program, 2025-MSLH-107).

Institutional Review Board Statement: Not applicable.

Informed Consent Statement: Not applicable.

Data Availability Statement: The original contributions presented in the study are included in the article, further inquiries can be directed to the corresponding author.

Conflicts of Interest: Authors Youfang Gu, Yu Song, Minkun He, JunChen Li, Shun Yang, XinYue Li and Yao Zhao were employed by the company China Southern Power Grid Co., Ltd. The authors declare that this study received funding from China Southern Power Grid Co., Ltd. The funder was not involved in the study design, collection, analysis, interpretation of data, the writing of this article or the decision to submit it for publication.

References

1. Mebrat, M.Y.; Ahmed, M.W.; Ectors, W. Business applications of cargo drones in the EU. *Transp. Res. Procedia* **2025**, *84*, 448–455. [CrossRef]
2. Jin, Z.; Ng, K.K.H.; Zhang, C.; Chan, J.J.; Qin, Y. A multistage stochastic programming approach for drone-supported last-mile humanitarian logistics system planning. *Adv. Eng. Inform.* **2025**, *65*, 103201.

3. Lu, Y.; Yang, J.; Yang, C. A humanitarian vehicle routing problem synchronized with drones in time-varying weather conditions. *Comput. Ind. Eng.* **2023**, *184*, 109563. [CrossRef]
4. Kumbhani, C.; Kant, R.; Shankar, R. Prioritizing sustainable solutions to mitigate risks in drone-based last-mile delivery. *Sustain. Futur.* **2025**, *9*, 100536.
5. Ropero, F.; Muñoz, P.; R-Moreno, M.D. TERRA: A path planning algorithm for cooperative UGV–UAV exploration. *Eng. Appl. Artif. Intell.* **2019**, *78*, 260–272. [CrossRef]
6. Jung, S. MILP-based cost and time-competitive vehicle routing problem for last-mile delivery service using a swarm of UAVs and UGVs. *J. Air Transp. Manag.* **2025**, *124*, 102736.
7. Kuo, R.J.; Lu, S.H.; Lai, P.Y.; Mara, S.T.W. Vehicle routing problem with drones considering time windows. *Expert Syst. Appl.* **2022**, *191*, 116264. [CrossRef]
8. Fan, H.; Sun, X.; Zhang, Y.; Ren, X.; Tian, P. Vehicle Path Problem with Mixed Time Window under Time-varying Road Network. *Comput. Eng. Appl.* **2022**, *58*, 292–302.
9. Sushma, M.B.; Mashhoodi, B.; Tan, W.; Liujiang, K.; Xu, Q. Spatial drone path planning: A systematic review of parameters and algorithms. *J. Transp. Geogr.* **2025**, *125*, 104209. [CrossRef]
10. Dorling, K.; Heinrichs, J.; Messier, G.G.; Magierowski, S. Vehicle routing problems for drone delivery. *IEEE Trans. Syst. Man. Cybern. Syst.* **2016**, *47*, 70–85. [CrossRef]
11. Kong, J.; Wang, H.; Xie, M. Autonomous delivery vehicle routing problem with drones based on multiple delivery modes. *Comput. Oper. Res.* **2025**, *179*, 107032. [CrossRef]
12. Mahmoudi, B.; Eshghi, K. Energy-constrained multi-visit TSP with multiple drones considering non-customer rendezvous locations. *Expert Syst. Appl.* **2022**, *210*, 118479.
13. Ghiani, G.; Guerriero, E.; Manni, E.; Pareo, D. Combining autonomous delivery robots and traditional vehicles with public transportation infrastructure in last-mile distribution. *Comput. Ind. Eng.* **2025**, *203*, 111001. [CrossRef]
14. Baldisseri, A.; Siragusa, C.; Seghezzi, A.; Mangiaracina, R.; Tumino, A. Truck-based drone delivery system: An economic and environmental assessment. *Transp. Res. Part D Transp. Environ.* **2022**, *107*, 103296. [CrossRef]
15. Wu, Y.; Wu, S.; Hu, X. Cooperative path planning of UAVs & UGVs for a persistent surveillance task in urban environments. *IEEE Internet Things J.* **2020**, *8*, 4906–4919. [CrossRef]
16. Murray, C.C.; Chu, A.G. The flying sidekick traveling salesman problem: Optimization of drone-assisted parcel delivery. *Transp. Res. Part C Emerg. Technol.* **2015**, *54*, 86–109. [CrossRef]
17. Liu, Y.; Liu, Z.; Shi, J.; Wu, G.; Pedrycz, W. Two-echelon routing problem for parcel delivery by cooperated truck and drone. *IEEE Trans. Syst. Man. Cybern. Syst.* **2020**, *51*, 7450–7465.
18. Boysen, N.; Briskorn, D.; Fedtke, S.; Schwerdfeger, S. Drone delivery from trucks: Drone scheduling for given truck routes. *Networks* **2018**, *72*, 506–527. [CrossRef]
19. Agatz, N.; Bouman, P.; Schmidt, M. Optimization approaches for the traveling salesman problem with drone. *Transp. Sci.* **2018**, *52*, 965–981. [CrossRef]
20. Yurek, E.E.; Ozmutlu, H.C. Traveling salesman problem with drone under recharging policy. *Comput. Commun.* **2021**, *179*, 35–49. [CrossRef]
21. Wang, Y.; Wang, Z.; Hu, X.; Xue, G.; Guan, X. Truck–drone hybrid routing problem with time-dependent road travel time. *Transp. Res. Part C Emerg. Technol.* **2022**, *144*, 103901.
22. Ye, F.; Chen, J.; Tian, Y.; Jiang, T. Cooperative task assignment of a heterogeneous multi-UAV system using an adaptive genetic algorithm. *Electronics* **2020**, *9*, 687. [CrossRef]
23. Lichau, S.; Sadykov, R.; François, J.; Dupas, R. A branch-cut-and-price approach for the two-echelon vehicle routing problem with drones. *Comput. Oper. Res.* **2025**, *173*, 106869. [CrossRef]
24. Gao, J.; Zhen, L.; Laporte, G.; He, X. Scheduling trucks and drones for cooperative deliveries. *Transp. Res. Part E Logist. Transp. Rev.* **2023**, *178*, 103267. [CrossRef]
25. Yue, W.; Li, B.; Zhang, X.; Yang, Q. HDFOS: Path planning for heterogeneous truck-drone cooperative delivery and pickup services. *Intel. Serv. Robot.* **2025**, *18*, 775–798. [CrossRef]
26. Croella, A.L.; Fraccascia, L. A location-sizing and routing model for a biomethane production chain fed by municipal waste. *Comput. Ind. Eng.* **2024**, *198*, 110714. [CrossRef]